Polymer 49 (2008) 3928–3937

Contents lists available at ScienceDirect

Polymer

journal homepage: www.elsevier.com/locate/polymer

Preparation of brush-like crystals of poly[2,6-(1,4-phenylene)-benzobisimidazole]

Jin Gong, Shin-ichiro Kohama, Kazuya Kimura, Shinichi Yamazaki, Kunio Kimura*

Graduate School of Environmental Science, Okayama University, 3-1-1 Tsushima-naka, Okayama 700-8530, Japan

ARTICLE INFO

Article history:
Received 3 June 2008
Received in revised form 7 July 2008
Accepted 11 July 2008
Available online 16 July 2008

Keywords:
Polybenzimidazole
Brush-like crystals
Morphology

ABSTRACT

Poly[2,6-(1,4-phenylene)-benzobisimidazole] (PPBI) crystals were prepared by using reaction-induced crystallization of oligomers during solution polymerization of 1,2,4,5-tetraaminobenzene and diphenyl terephthalate. Polymerizations were carried out at a monomer concentration of 4.3×10^{-2} mol L^{-1} at 350 °C for 6 h. Brush-like PPBI crystals were obtained in a mixture of structural isomers of dibenzyltoluene, in which many needle-like crystals came out vertically from the surface of the ribbon-like crystals. Average width and thickness of the ribbon-like crystals were 0.75 μm and 0.11 μm, respectively. And average length and diameter of the needle-like crystals were 0.36 μm and 50 nm, respectively. The brush-like crystals possessed high crystallinity and exhibited good thermal resistance. The ribbon-like crystals were formed by the crystallization of imidazole oligomers at an initial stage of polymerization, and then the needle-like crystals grew from the surface of the ribbon-like crystals. Polymerization occurred on the crystals when the oligomers were crystallized, leading to the high molecular weight PPBI crystals.

1. Introduction

Polybenzimidazoles are aromatic heterocyclic polymers being notable as high-performance polymers [1,2] and some of them are commercially used as heat-resistant materials. The fully aromatic nature and stiffness of molecular chains endue them with superior properties such as thermal stability, mechanical strength, chemical resistance and so on. However, their molecular structures also bring about intractability [3]. Poly[2,6-(1,4-phenylene)-benzobisimidazole] (PPBI) which is a representative of polybenzimidazole has a straight and planar molecular structure, and it is supposed to be one of the most ideal high-performance materials. PPBI does not melt under decomposition and it is soluble only in strong acids such as concentrated sulfuric acid and methanesulfonic acid. Therefore, it possesses the same perplexing problem of high performance versus tractability. Many efforts have been launched to overcome this antagonistic problem. The efforts to improve their processability have been generally directed toward the chemical modification of polymer backbones including the substituting at the reactive N–H sites in imidazole moiety [4–9]. However, the structural modification always imparts solubility at the cost of sacrificing the desirable properties derived from wholly aromatic polymer structure.

We have been studying morphology control of intractable aromatic polymers by using reaction-induced phase separation of oligomers during solution polymerization [10–17]. These studies demonstrated that the reaction-induced phase separation of oligomers was a useful method to overcome the trade-off problem between high performance and poor processability. In this paper, morphology control of PPBI was examined by using the reaction-induced phase separation of oligomers during solution polymerization of 1,2,4,5-tetraaminobenezene (TAB) and diphenyl terephthalate (DPTP) as shown in Scheme 1.

2. Experimental section

2.1. Materials

DPTP was purchased from Wako Pure Chemical Co. Ltd. and recrystallized from ethyl acetate. Diphenyl sulfone (DPS) was purchased from Aldrich Co. Ltd. and recrystallized from a mixture of methanol and water. A mixture of structural isomers of dibenzyltoluene (DBT) was purchased from Matsumura oil Co. Ltd. (Trade name was Barrel Therm 400, MW: 380, b.p. 382 °C) and purified by vacuum distillation (180–200 °C/0.3 mmHg). Liquid paraffin (LPF) was purchased from Nacalai Tesque Co. Ltd. and purified by vacuum distillation (220–240 °C/0.3 mmHg). Number average molecular

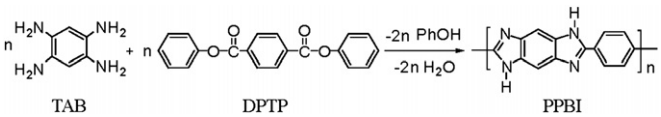

Scheme 1. Synthesis of PPBI from TAB and DPTP.

* Corresponding author. Tel./fax: +81 86 251 8902.
E-mail address: polykim@cc.okayama-u.ac.jp (K. Kimura).

0032-3861/$ – see front matter © 2008 Elsevier Ltd. All rights reserved.
doi:10.1016/j.polymer.2008.07.011

Table 1
Synthesis of PPBI in various solvents

Run no.	Solvent	Yield (%)	η_{inh}[a] (dL g^{-1})	Morphology	Average size				$T_{5\%}$[c] (°C)
					Width ($\times 10^{-1}$ μm)	cv[b] (%)	Thickness ($\times 10^{-1}$ μm)	cv (%)	
1	LPF	35	0.61	Brush	5.2	47	1.5	33	460
2	DBT	81	0.58	Brush	7.5	25	1.1	30	531
3	DBT/DPS-50	87	0.76	Ribbon	4.3	27	0.7	40	374
4	DPS	97	–[d]	Fiber	1.0[e]	32	–	–	332

[a] η_{inh} was measured in 97% sulfuric acid at a concentration of 0.2 g dL^{-1} at 30 °C.
[b] Coefficient of variation.
[c] Temperature of 5% weight loss measured on a TGA at a heating rate of 20 °C min^{-1} in N_2.
[d] Not measured because the precipitates were insoluble.
[e] Average diameter of fiber.

weight of LPF was 930 and tertiary carbon content was 15% evaluated by ^{13}C NMR spectroscopy according to previous reports [18–20]. 1,2,4,5-Tetraaminobenezene tetrahydrochloride (TAB·4HCl) was purchased from Aldrich Co. Ltd. and recrystallized from deaerated water. TAB was prepared from TAB·4HCl according to a previous procedure [21].

2.2. Measurements

Infrared (IR) spectra were recorded on a JASCO FT/IR-410 spectrometer. Inherent viscosity (η_{inh}) was measured in 97% sulfuric acid at a concentration of 0.2 g dL^{-1} at 30 °C. Morphologies and sizes of the products were observed on a Hitachi S-3500N scanning electron microscope (SEM). Samples for SEM observation were dried, sputtered with platinum/palladium and observed at 20 kV. Average size parameters of the products were determined by taking the average of over 150 observation values. Thermogravimetric analysis (TGA) was performed on a Perkin–Elmer TGA-7A with a heating rate of 20 °C min^{-1} in nitrogen. Wide angle X-ray scattering (WAXS) was performed on a RIGAKU MiniFlex diffractometer with nickel-filtered Cu Kα radiation at a scanning rate of 1° min^{-1}. Matrix assisted laser desorption ionization time-of-flight (MALDI-TOF) mass spectrometry were performed on a Bruker Daltonics AutoFLEX MALDI-TOF MS system operating with a 337-nm N_2 laser. Spectra were obtained in the linear positive mode with an accelerating potential of 20 kV. Mass calibration was performed with angiotensin I (MW 1296.69) and insulin B (MW 3496.96) from a Sequazyme peptide mass standard kit. Samples were prepared by the evaporation–grinding method and ran in 3-aminoquinoline as a matrix doped with potassium trifluoroacetate salt according to previously reported procedures [22,23].

2.3. Polymerization

Polymerization in DBT was described as a typical example. DPTP (0.27 g, 0.86 mmol) and 20 ml of DBT were placed into a cylindrical flask equipped with gas inlet and outlet tubes. The reaction mixture was heated up to 350 °C under slow stream of nitrogen with stirring. When DPTP was entirely dissolved in DBT during heating, TAB (0.12 g, 0.86 mmol) was added at 350 °C into this solution. The solution was stirred for 5 s to dissolve TAB, and then polymerization was carried out for 6 h at 350 °C without stirring. Precipitated

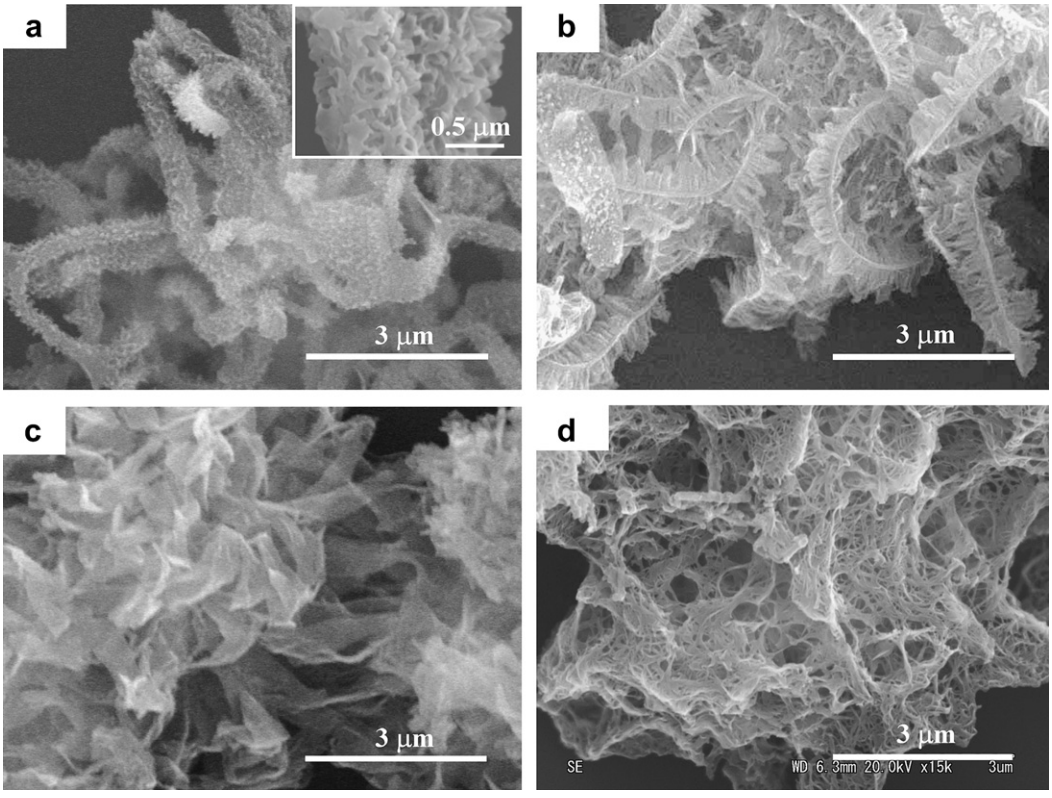

Fig. 1. Morphologies of products prepared in (a) LPF, (b) DBT, (c) DBT/DPS-50 and (d) DPS for 6 h.

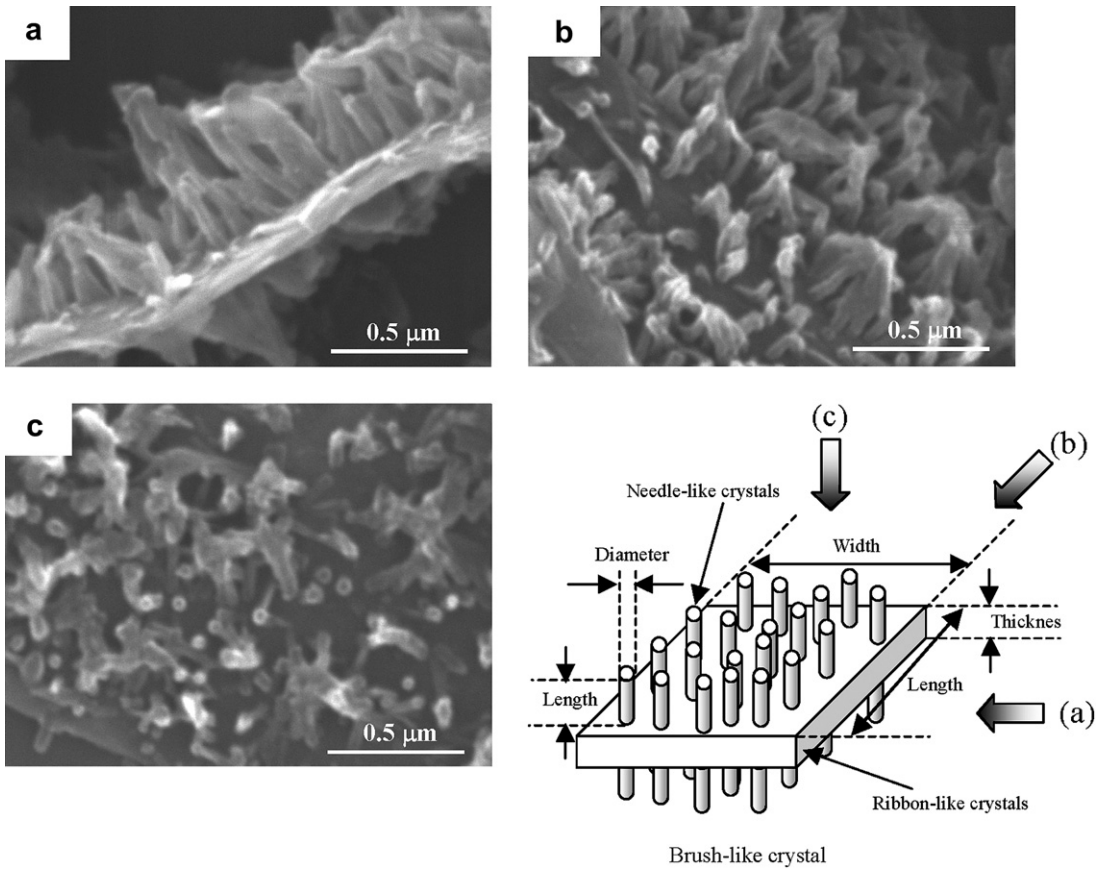

Fig. 2. Micrographs of brush-like crystals taken from three different directions. The crystals were prepared in DBT for 6 h.

polymers were isolated by filtration at 350 °C to avoid the precipitation of oligomers on the crystals during cooling, and then washed with acetone. PPBI crystals were obtained with the yield of 81%. A filtrate was poured into *n*-hexane and precipitated oligomers which were dissolved in DBT at 350 °C were collected by filtration. Polymerizations in other solvents were carried out in the similar manner.

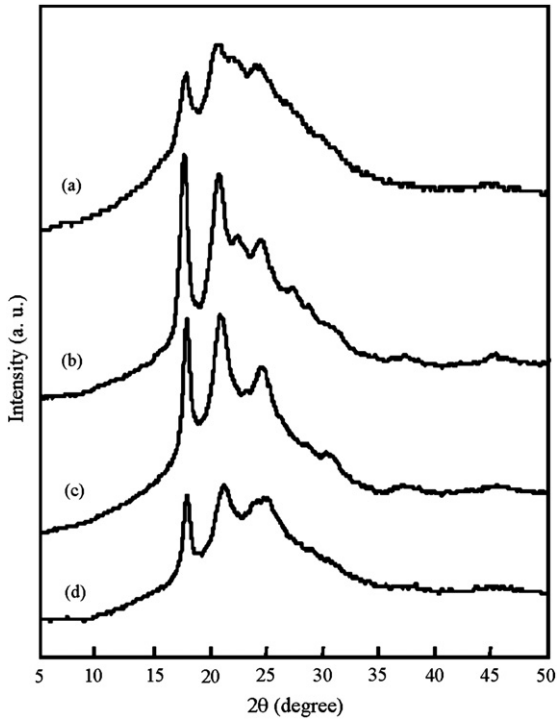

Fig. 3. WAXS patterns of products prepared in (a) LPF, (b) DBT, (c) DBT/DPS-50 and (d) DPS for 6 h.

3. Results and discussion

3.1. Influence of solvent on morphology

Poor solvents to PPBI are necessary to induce the phase separation of oligomers during solution polymerization, and morphology of the precipitates is usually influenced by the solubility of oligomers [24]. Polymerizations were carried out in LPF, DBT, DBT/DPS-50 (content of DPS was 50 wt%) and DPS at

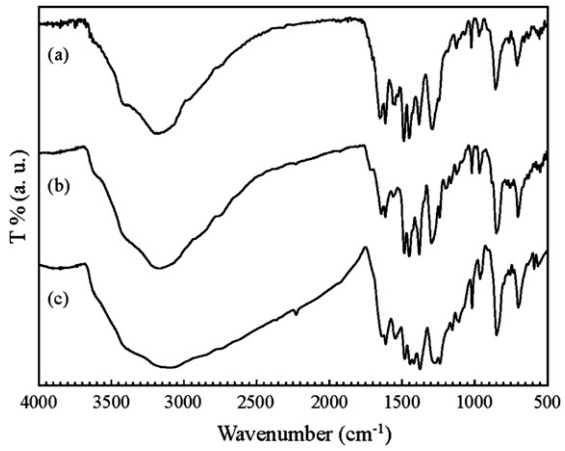

Fig. 4. IR spectra of crystals prepared in (a) LPF, (b) DBT and (c) DPS for 6 h.

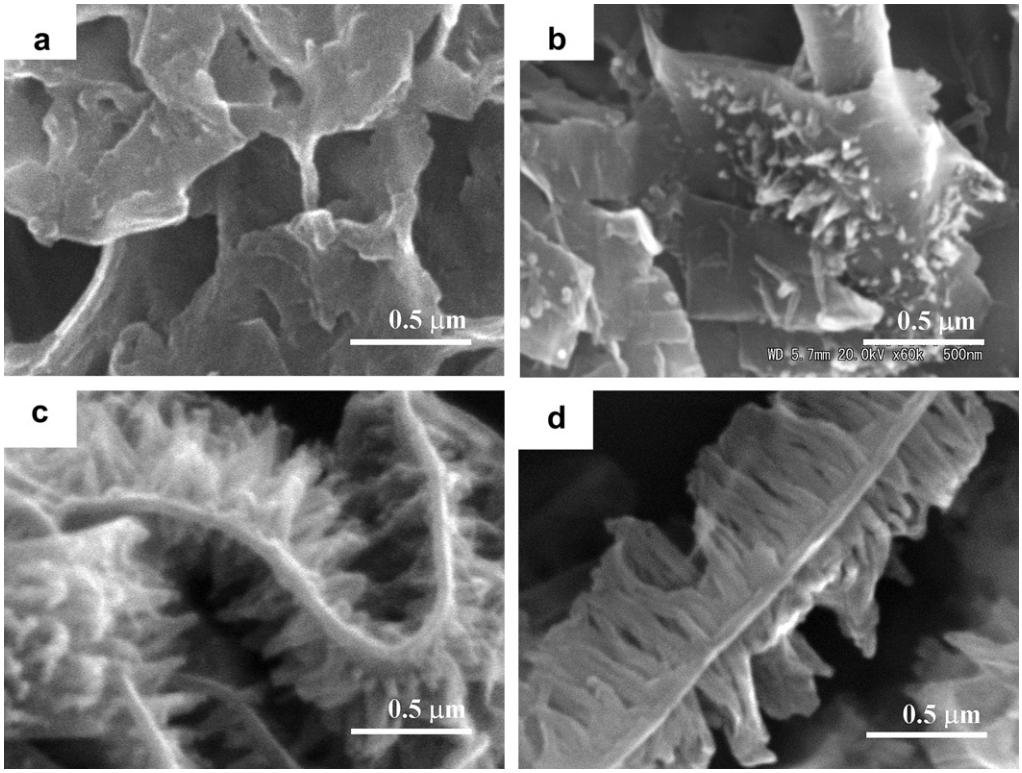

Fig. 5. Micrographs of crystals prepared in DBT for (a) 0.5 h, (b) 1 h, (c) 3 h and (d) 21 h.

a monomer concentration of 4.3×10^{-2} mol L^{-1} at 350 °C. This monomer concentration is corresponding to 1% based on the calculated polymer weight. Both monomers were insoluble in these solvents at room temperature, but they were dissolved during heating. DPTP was less soluble than TAB into these solvents, and therefore DPTP was first heated with the solvent. Then TAB was

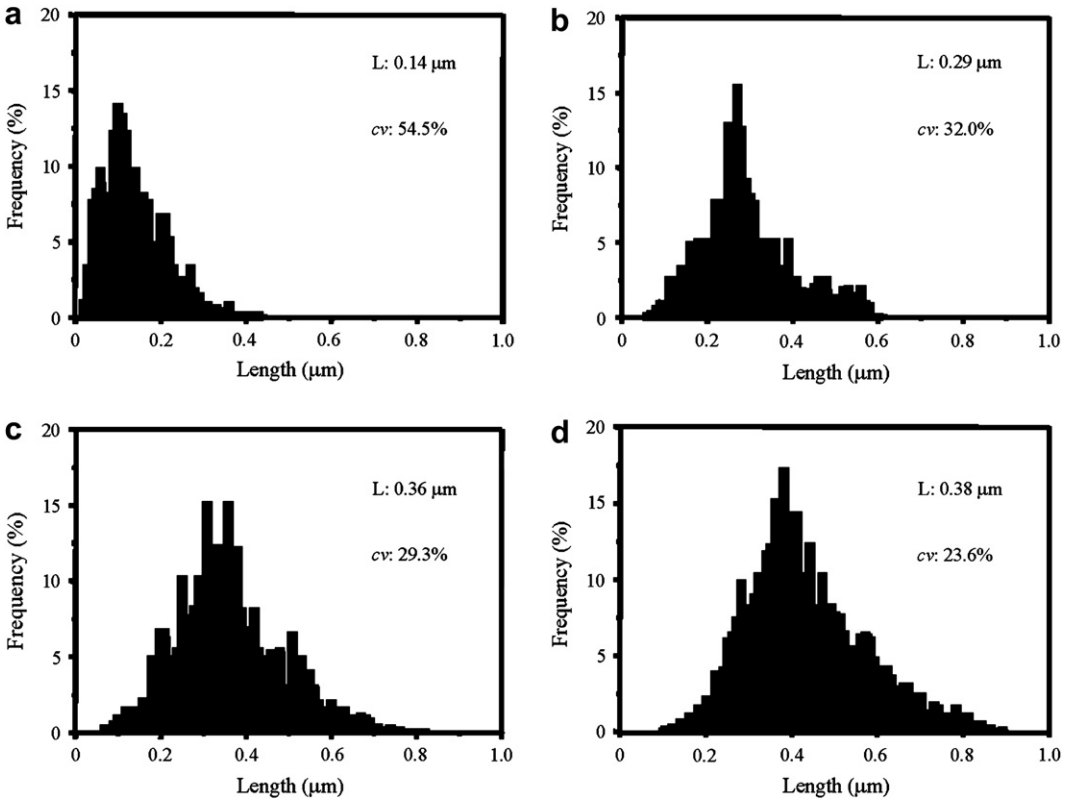

Fig. 6. Distribution diagrams of length of needle-like crystals on brush-like crystals prepared in DBT for (a) 1 h, (b) 3 h, (c) 6 h and (d) 21 h. *L* and cv denote average length and coefficient of variation, respectively.

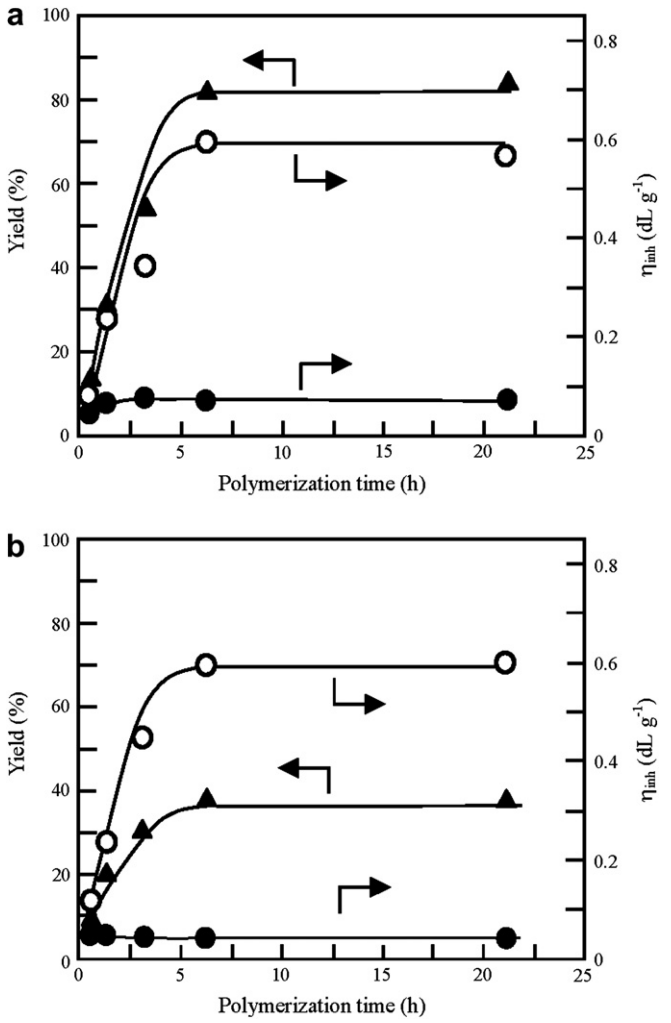

Fig. 7. Plots of yield (▲), inherent viscosity of crystals (○) and oligomers recovered from solution (●) as a function of polymerization time. Polymerizations were carried out in (a) DBT and (b) LPF.

added into the DPTP solution after DPTP was entirely dissolved. After an addition of TAB, the solution became turbid and PPBI precipitates were obtained after 6 h. Polymerization results are presented in Table 1. Morphology of the PPBI precipitates was drastically changed with the solvent. Brush-like crystals were obtained in LPF with the yield of 32%. Average width and thickness were 0.52 μm and 0.15 μm, and their coefficients of variation (cv) were 47% and 33%, respectively. Many protuberances were formed on the surfaces of the crystals as shown in Fig. 1(a). It was difficult to measure the length of the brush-like crystals because of their entanglement, but the length was longer than 15 μm. Sublimation of monomers from LPF solution lowered the yield. In DBT, the precipitated crystals exhibited also brush-like morphology as shown in Fig. 1(b). SEM images of the brush-like crystals taken from three different directions are shown in Fig. 2. They were comprised of ribbon-like crystals and needle-like crystals. Definitions of length, width and thickness of the ribbon-like crystals, and length and diameter of the needle-like crystals are depicted in Fig. 2. Average length of the ribbon-like crystals could not be also measured because of their entanglement, it was also longer than 10 μm. Average width and thickness of the ribbon-like crystals were 0.75 μm and 0.11 μm, respectively. Their cv values were 25% and 30%. Many needle-like crystals came out perpendicularly from both surfaces of the ribbon-like crystals, and average length and diameter of the needle-like crystals were 0.36 μm and 50 nm, respectively. Average number of the needle-like crystals in the square micrometers of the surface area of the ribbon-like crystal was 55. The brush-like crystal prepared in DBT possessed longer needle-like crystals than those prepared in LPF. In contrast to this, ribbon-like crystals having smooth surface were also formed in DBT/DPS-50 with the yield of 87%, as shown in Fig. 1(c), of which average width and thickness were 0.43 μm and 70 nm with the cv values of 27% and 40%. Entangled fibrils were obtained in DPS with the yield of 97%, as shown in Fig. 1(d), of which average diameter was 0.1 μm with the cv values of 32%. The values of η_{inh} of the precipitated crystals prepared in LPF, DBT and DBT/DPS-50 were 0.61 dL g^{-1}, 0.58 dL g^{-1} and 0.76 dL g^{-1}, being comparable to those previously prepared by solution polymerization [25]. These precipitated crystals were high molecular weight polymers. Entangled fibrils obtained in DPS were insoluble even in sulfuric acid. WAXS patterns of the precipitates were measured as shown in Fig. 3. The sharp reflection peaks were observed at 2θ of 17.8°, 20.8°, 22.5° and 24.5° in the profile of the brush-like crystals formed in DBT. The brush-like crystals prepared in DBT possessed the highest crystallinity. Relative peak intensities of these reflections toward diffuse hallo contributed from amorphous regions became lower from DBT to DPS with the increase of the content of DPS in the solvent. Even

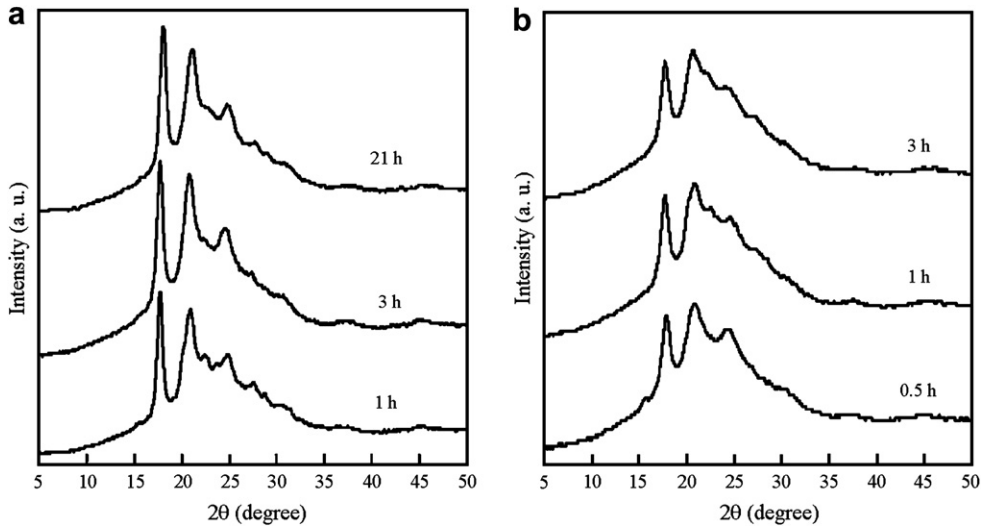

Fig. 8. WAXS intensity profiles of PPBI crystals prepared in (a) DBT and (b) LPF for different time.

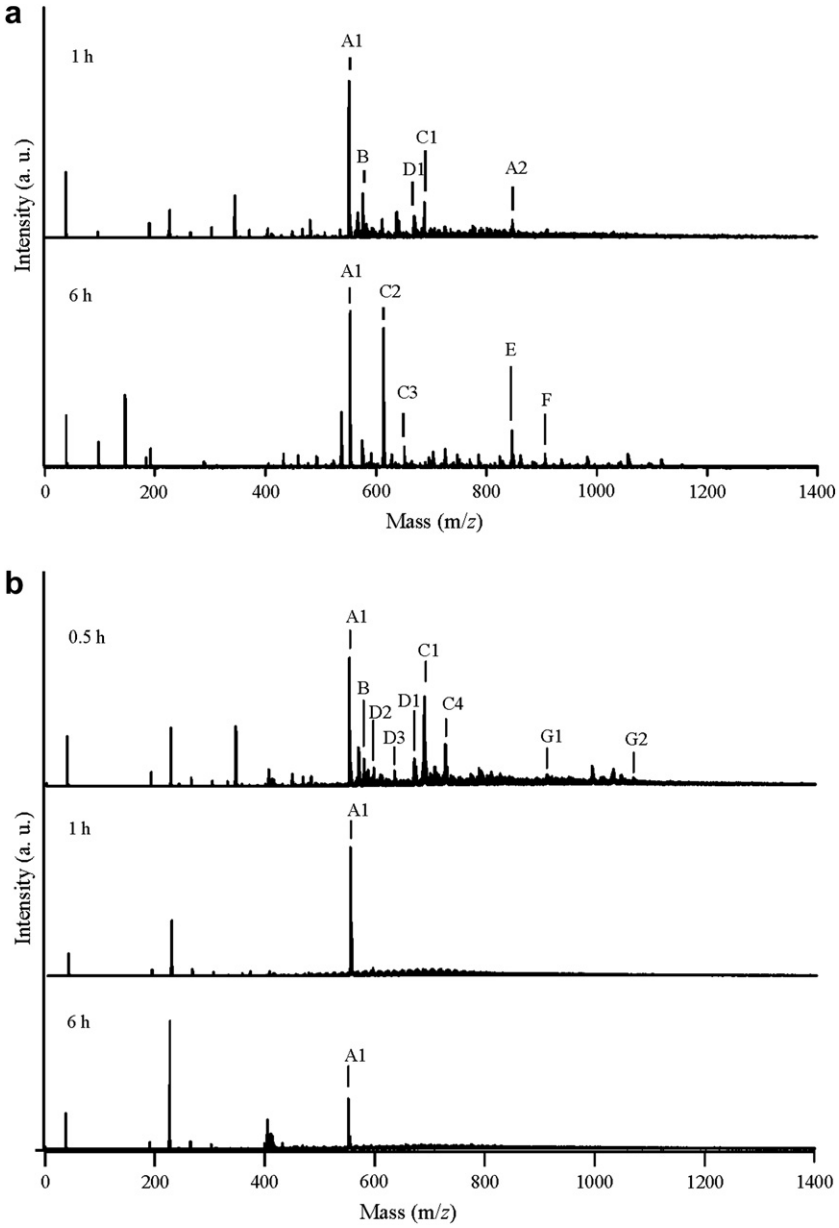

Fig. 9. MALDI-TOF mass spectra of PPBI oligomers collected from solution. Polymerization was carried out in (a) DBT and (b) LPF for different time periods.

though the morphology was quite similar, the brush-like crystals prepared in LPF possessed the lowest crystallinity. IR spectra of crystals prepared in LPF, DBT and DPS are shown in Fig. 4. In the spectra of the brush-like crystals prepared in LPF and DBT, the characteristic peaks of PPBI were clearly observed at 3500–3000 cm^{-1} (N–H and aromatic C–H stretching), 1640 cm^{-1} (C═N stretching of imidazole ring) and 1612 cm^{-1} (C═N stretching of imidazole ring), 1375 cm^{-1} (ring vibration of imidazole), and the formation of PPBI was confirmed. In contrast to this, unassignable peaks were observed at 1415 cm^{-1} and 1273 cm^{-1} in the spectrum of the precipitates in DPS besides the characteristic peaks of PPBI, which were not the uncyclized precursors.

Thermal stability of the precipitates was evaluated by TGA in nitrogen. Temperatures of 5% weight loss ($T_{5\%}$) of the brush-like crystals prepared in LPF and DBT were 460 °C and 531 °C, also presented in Table 1. Although $T_{5\%}$ of the crystals prepared in LPF was inferior, these crystals exhibited good thermal stability. However, $T_{5\%}$s of the precipitates prepared in DBT/DPS-50 and DPS were 374 °C and 332 °C, respectively, and they were significantly lower. The results of WAXS, IR, viscosity measurements and TGA suggested that the polymers prepared in the solvent contained DPS might contain the structural defects formed by the undesirable side reaction, bringing about the cross-linking structure. The monomers probably reacted with DPS, but true nature of the side reaction remained unclear.

3.2. Formation of brush-like crystals

In order to examine the formation mechanism of the brush-like crystals, morphology of the precipitates was observed in the course of polymerization in DBT. As shown in Fig. 5, aggregates of plate-like or ribbon-like crystals were formed after 0.5 h. The surface of these crystals was very smooth and protuberances were not observed. The protuberances appeared on the surface after 1 h and their length increased leading to the formation of the needle-like crystals on the surface. Then the brush-like crystals were formed after 3 h. The length distributions of the needle-like crystals were evaluated with their cv values as shown in Fig. 6. All

Table 2
Assignments of peaks in the MALDI-TOF mass spectra of Fig. 9(a)

Peak code	Mass (m/z)			Structure	*n*	Cation
	Measured		Calculated			
	1 h	6 h				
A1	551.40	552.01	551.58	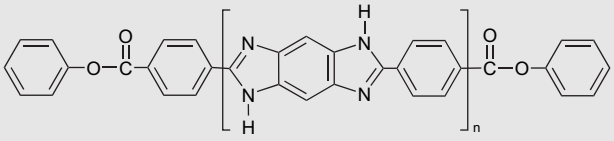	1	H^+
A2	848.18	–	846.96		2	K^+
B	577.56	–	577.63	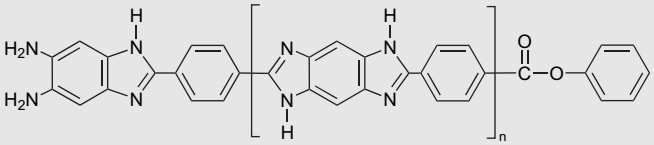	1	H^+
C1	687.83	–	688.85	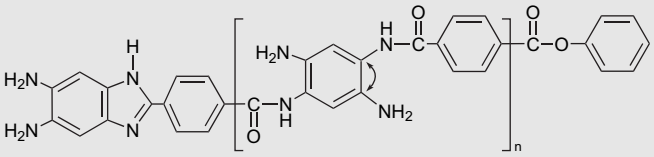	1	K^+K^+
C2	–	612.28	613.66		1	H^+
C3	–	650.38	650.75		1	K^+
D1	669.74	–	670.84	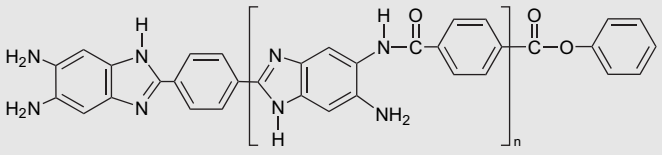	1	K^+K^+
E[a]	–	845.00	845.91	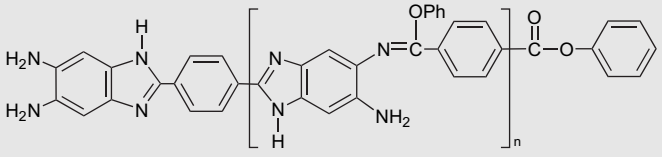	2	H^+
F[a]	–	905.14	905.19	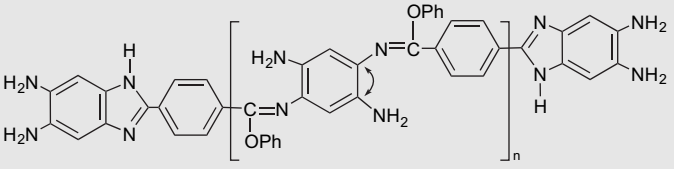	1	$K^+K^+K^+$

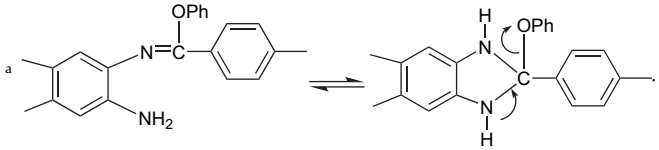

these distributions exhibit unimodality. Average length was 0.14 μm with the cv value of 54.5% after 1 h and 0.29 μm with the cv value of 32.0% after 3 h. Then it increased gradually to 0.36 μm with the cv value of 29.3% after 6 h. Afterward, it became constant at 0.38 μm with the cv value of 23.6% until 21 h. The increase in length is corresponding to that in yield of the crystals as discussed below, indicating that the needle-like crystals grew by the precipitation of the oligomers. The width and the thickness of the ribbon-like crystals were almost constant at 0.75 μm and 0.11 μm throughout the polymerization. Yield and η_{inh} of the crystals and the oligomers collected from solution were examined during polymerization. As shown in Fig. 7, the yield increased with polymerization time and then it became constant after 6 h. This reveals that the crystals were grown by the consecutive supply of oligomers precipitated from solution as aforesaid. The value of η_{inh} of the crystals also increased with polymerization time until 6 h, and then leveled off. In contrast to this, the value of η_{inh} of the oligomers was almost constant throughout the polymerization. These results implied that when the molecular weight of oligomers exceeded a critical value, they were precipitated via supersaturated state to form the crystals. Condensation reaction occurred effectively on the crystals when the oligomers were crystallized.

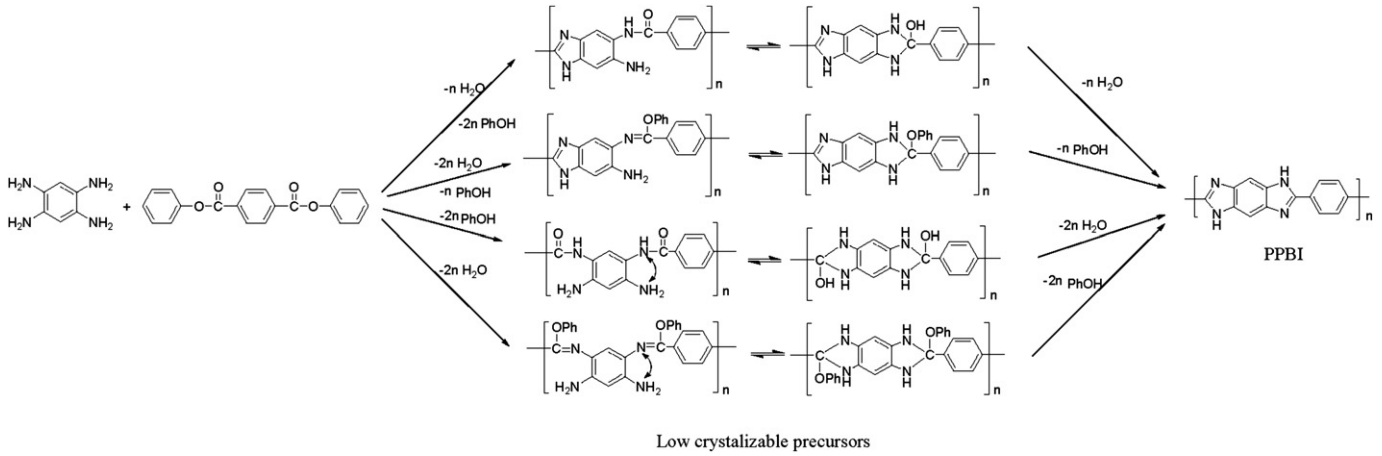

Scheme 2. Reaction mechanism of PPBI.

The fact that the molecular weight of polymers became constant after the yield was leveled off exhibits that the solid-state polymerization hardly occurred in the crystals because of the low mobility of molecular chains in the crystals. WAXS profiles of these crystals are shown in Fig. 8. The crystallinity of crystals prepared for 1 h was as high as that of crystals prepared for 21 h. This result strongly supports the above discussion that the PPBI brush-like crystals were formed by the crystallization of the oligomers. In order to make the structure of the precipitated oligomers clear, the oligomers dissolved in the solution were collected after 1 h and 6 h, and analyzed by the MALDI-TOF mass spectrometry. The spectra are shown in Fig. 9(a) and the peaks identified are listed in Table 2. The recovered compounds contained one or two repeating units, indicating that the precipitated oligomers might be mainly more than trimers. The imidazole oligomers were detected both after 1 h and 6 h. Because of the straight, rigid and planar structure of the imidazole oligomers, they can crystallize to form the clear morphology. On the contrary, the uncyclized oligomers would prevent to form the crystal because of the structure irregularity and the structural defects, as shown in Scheme 2. Further, it is also noticed that the content of the imidazole oligomers became lower with the polymerization time, and the imidazole oligomers were preferably precipitated due to the lower solubility in DBT than the uncyclized oligomers. Molecular orientation in the brush-like crystals could not be estimated by X-ray or electron diffraction because the crystal lattice parameters have not been determined. Therefore, the formation mechanism of the brush-like crystals could not be clarified. Based on the unique morphology, it might be

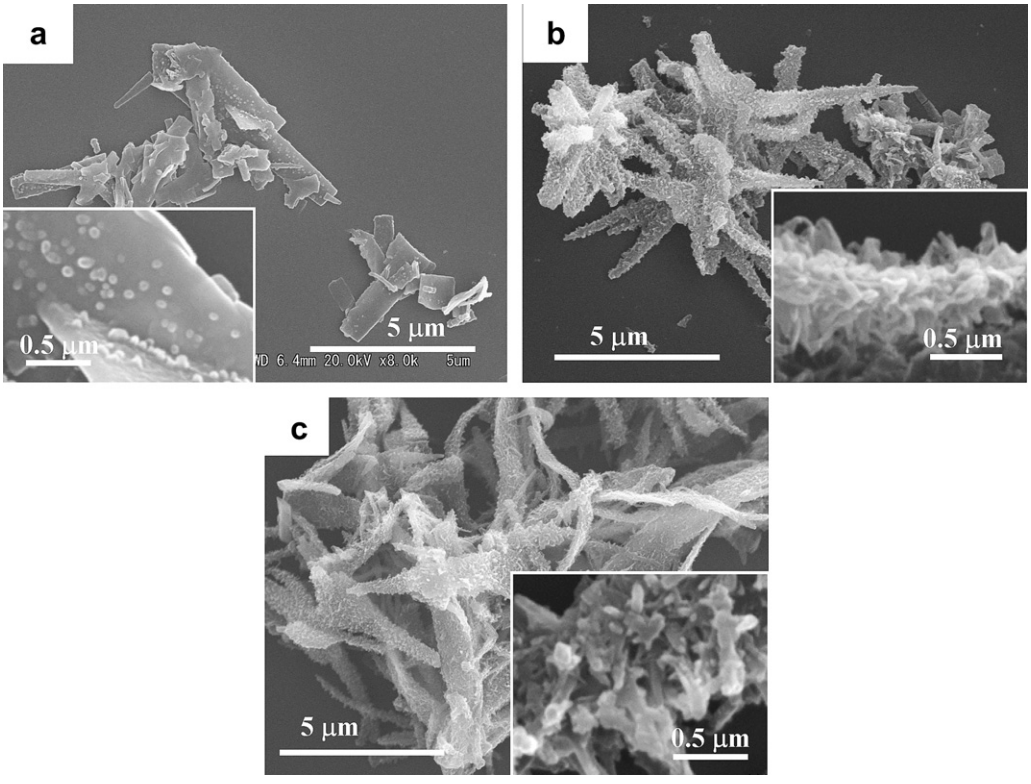

Fig. 10. Morphologies of products prepared in LPF for (a) 0.5 h, (b) 1 h and (c) 3 h.

Table 3
Assignments of peaks in the MALDI-TOF mass spectra of Fig. 9(b)

Peak code	Mass (m/z)				Structure	n	Cation
	Measured			Calculated			
	0.5 h	1 h	6 h				
A1	551.54	551.12	551.61	551.58	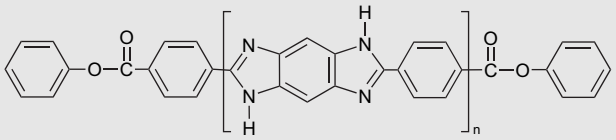	1	H^+
B	577.56	–	–	577.63	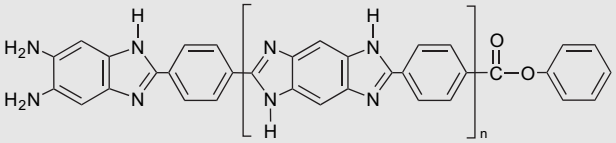	1	H^+
C1	687.95	–	–	688.85	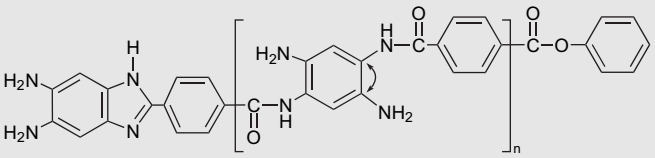	1	K^+ K^+
C4	726.00	–	–	726.95		1	$K^+K^+K^+$
D1	669.90	–	–	670.84	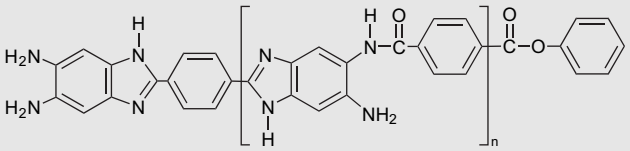	1	K^+K^+
D2	595.70	–	–	595.65		1	H^+
D3	633.75	–	–	632.74		1	K^+
G1	910.42	–	–	911.10	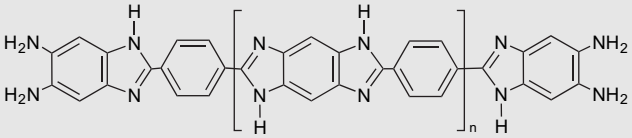	2	K^+K^+
G2	1068.70	–	–	1068.15		3	H^+

speculated that the brush-like crystals were formed by the homoepitaxial crystallization previously reported in the crystallization of poly(aryl ether ketone), polyimides and others [26–31]. Low molecular weight oligomers form the ribbon-like crystals at the initial stage in the polymerization, and then higher molecular weight oligomers crystallize to form the needle-like crystals epitaxially on the plate-plane of the ribbon-like crystals with polymerization time. Alternatively, cilia formed on the surface of the ribbon-like crystals by the distribution of the molecular length of the precipitated oligomers might afford the crystal growth step to form the needle-like crystals reported in the crystallization of poly(*p*-phenylene benzobisthiazole) [32].

The brush-like crystals were also obtained in LPF, but they did not exhibit the high crystallinity as aforesaid. In order to clarify the difference, yield and η_{inh} of the crystals and the oligomers collected from solution were examined during polymerization in LPF. As shown in Fig. 7, the yield increased with polymerization time and then it became constant after 6 h. The value of the η_{inh} of the crystals also increased with the polymerization until 6 h, and then leveled off. This tendency is similar to that in DBT. Although the value of the η_{inh} of the oligomers was almost constant throughout the polymerization in LPF as well as in DBT, the value of the η_{inh} was lower than that in DBT. With respect to morphology, the ribbon-like crystals were formed after 0.5 h as shown in Fig. 10. Many protuberances were observed on the surface of these ribbon-like crystals. Then the length of these protuberances increased to form the needle-like crystals on the surface in the same manner as those prepared in DBT. WAXS profiles of these crystals are shown in Fig. 8. Although the reflection peaks were observed at 2θ of 17.9°, 20.6° and 24.1° in the pattern of incipient crystals prepared for 0.5 h, these peaks were not as sharp as those prepared in DBT. The peak intensity relative to the diffuse hallo contributed from amorphous regions was lower than that prepared in DBT. And the crystallinity gradually lowered with polymerization time. The oligomers collected from the solution after 0.5 h, 1 h and 6 h were analyzed by the MALDI-TOF mass spectrometry. The spectra are shown in Fig. 9(b) and the peaks identified are listed in Table 3. Various oligomers such as cyclized imidazole oligomers and uncyclized oligomers existed in the solution after 0.5 h. In contrast to the results in DBT, it should be noted that uncyclized oligomers were not detected after 1 h and the only oligomer dissolved in the solution was the cyclized imidazole oligomer end-capped by phenyl ester. This result suggests that the uncyclized polar oligomers were also precipitated in LPF due to the lower solubility. As aforesaid, the uncyclized oligomers could not form good crystals because of the structure irregularity and the structural defects, and therefore the brush-like crystals prepared in LPF might possess the lower crystallinity.

4. Conclusions

The morphology of the PPBI crystals was significantly influenced by the solvent, and the brush-like PPBI crystals were prepared in DBT. They were the ribbon-like crystals having needle-like crystals came out from the surface. They showed high crystallinity and exhibited good thermal resistance. The ribbon-like crystals were formed by the crystallization of cyclized imidazole oligomers at an initial stage of polymerization and then the needle-like crystals grew on the surface of the ribbons. The polymerization occurred when the oligomers were crystallized, leading to the high molecular weight PPBI crystals. Although the brush-like crystals were also formed in LPF, their thermal stability and the crystallinity were not so high compared with those prepared in DBT. In LPF, uncyclized oligomers were precipitated to form the crystal due to their lower solubility. The solvent was an important parameter to control the morphology of PPBI crystals and DBT was the most suitable solvent to prepare the brush-like crystals.

References

[1] Cassidy PE. Thermally stable polymers, syntheses and properties. New York: Marcel Dekker; 1980.
[2] Korshak VV. Heat-resistant polymers. Israel Program for Scientific Translations, Jerusalem; 1971.
[3] Husman P, Helminiak T, Adams W. Resins for aerospace. ACS Symp Ser 1980; 132:203.
[4] Lammers M, Klop EA, Northolt MG, Sikkema DJ. Polymer 1998;39:5999.
[5] Jenkins S, Jacob IK, Polk BM, Kumar S, Dang TD, Arnold FE. Macromolecules 2000;33:8731.
[6] Dang TD, Arnold FE. Polym Prepr (Am Chem Soc Div Polym Chem) 1992;33(1): 912.
[7] Gieselman MB, Reynolds JR. Macromolecules 1992;25:4832.
[8] Sansone MJ. U.S. Patent 4,898,917; Feb 6 1990.
[9] Klaehn JR, Luther TA, Orme CJ, Jones MG, Wertsching AK, Peterson ES. Macromolecules 2007;40:7487.
[10] Kimura K, Yamashita Y. J Polym Sci Part A Polym Chem 1996;34:739.
[11] Kimura K, Nakajima N, Kobashi K, Yamashita Y, Yokoyama F, Uchida T, et al. Polym Adv Technol 2000;11:747.
[12] Kimura K, Kohoma S, Yamashita Y. Macromolecules 2002;35:7545.
[13] Kimura K, Kobashi K, Maeda H, Yamashita Y. Macromol Rapid Commun 2003; 24:190.
[14] Kumar SA, Kimura K, Yamsshita Y. J Appl Polym Sci 2003;88:1320.
[15] Kimura K, Inoue H, Kohama S, Yamashita Y, Sakaguchi Y. Macromolecules 2003;36:7721.
[16] Kobashi K, Kimura K, Yamashita Y. Macromolecules 2004;37:7570.
[17] Wakabayashi K, Kohama S, Yamazaki S, Kimura K. Polymer 2007;48:458.
[18] Freche P, Grenier-Loustalot MF, Gascoin A. Makromol Chem 1983;184:569.
[19] Dorman DE, Otocka EP, Bovey FA. Macromolecules 1972;5:574.
[20] Usami T, Takayama S. Macromolecules 1984;17:1756.
[21] Vogel H, Marvel CS. J Polym Sci 1961;50:511.
[22] Wakabayashi K, Uchida T, Yamazaki S, Kimura K, Shimamura K. Macromolecules 2007;40:239.
[23] Gies AP, Nonidez WK, Anthamatten M, Cook RC, Mays JW. Rapid Commun Mass Spectrom 2002;16:1903.
[24] Kimura K, Kohama S, Yamazaki S. Polym J 2006;38:1005.
[25] Kohama S, Gong J, Kimura K, Yamazaki S, Uchida T, Shimamura K, et al. Polymer 2008;49:1783.
[26] Fu L, Zhang S, Liu J, Wu Z, Yang D. Macromol Chem Phys 2001;202:2853.
[27] Lovinger AJ, Hudson SD, Davis DD. Macromolecules 1992;25:1252.
[28] Cheng SZD, Ho RM, Hsiao BS. Macromolecules 1996;177:185.
[29] Liu J, Cheng SZD, Harris FW, Hsiao BS, Gardner KH. Macromolecules 1994;27: 989.
[30] Wittmann JC, Lotzs B. Prog Polym Sci 1990;15:909.
[31] Cheng SDZ, Ho RM. Macromol Chem Phys 1996;191:185.
[32] Shimamura K, Uchida T. J Macromol Sci Phys 2000;B39(5):66.